Analytic and numerical study of stochastic resonance

Ronald F. Fox and Yan-nan Lu*
School of Physics, Georgia Institute of Technology, Atlanta, Georgia 30332-0430
(Received 10 May 1993)

A detailed analytic and numerical study of stochastic resonance in the regime of small-amplitude periodic modulation is presented. For the double-well potential, it has been suggested that the first-passage time for hopping from one potential minimum to the other is exactly half the modulation period at the value of the noise strength that maximizes the stochastic resonance profile. This explanation of the phenomenon is critically assessed. We establish a criterion for the noise strength at which the stochastic resonance profile is maximal.

PACS number(s): 05.40.+j, 02.50.−r

I. INTRODUCTION

Stochastic resonance was originally introduced to explain the periodicity of the Earth's ice ages [1]. Almost immediately, an experiment on a two-state Schmitt trigger circuit was reported [2]. Five years later, a second experiment with a ring laser was reported [3]. Since then, numerous theoretical papers have appeared and an entire issue of the Journal of Statistical Physics [4] was devoted to the proceedings of a stochastic resonance conference that covered many new applications.

What is stochastic resonance? This is not so easy to answer. It is not an ordinary resonance [5], and it requires very special circumstances. Presented in this introduction are the ideas required, before one can properly say what stochastic resonance is. The basic ideas can be introduced by examining a very simple system, the parabolic potential. This system does not exhibit stochastic resonance, but it does serve as the standard against which to judge for stochastic resonance, as will be done below for the double-well potential.

The governing equation in the parabolic potential case is

$$\frac{d}{dt}x = -\lambda x + a_0 \cos(\Omega t + \phi) \tag{1}$$

in which x is a dimensionless position variable, λ is the relaxation rate (we imagine, for later reference, that $\lambda = 1$ is taken at the end of a calculation), $a_0 \ll 1$ is the small amplitude of the periodic modulation, Ω is the modulation frequency ($\Omega \ll 1$), and ϕ is a uniformly distributed random phase. For stochastic resonance, we focus on the two-time position autocorrelation function, which, in this case, is

$$\{x(t)x(t')\} = \frac{1}{2}a_0^2 \frac{1}{\lambda^2+\Omega^2}\cos[\Omega(t-t')] \tag{2}$$

wherein the symbol $\{\ \}$ denotes averaging with respect to ϕ. The uniform phase average makes the averaged process "stationary" in the stochastic sense, which means dependent on $t-t'$ only (not on absolute t or t') and does not mean time independent. The Fourier transform of the autocorrelation is a function of ω. It has a term proportional to the Dirac delta function: $\delta(\omega-\Omega)$. The coefficient of this term is the amplitude of the Fourier transform at $\omega=\Omega$, and will be referred to below as the stochastic resonance amplitude (A_{SR}). For the parabolic potential,

$$A_{\mathrm{SR}} = \frac{\pi}{2}a_0^2 \frac{1}{\lambda^2+\Omega^2} . \tag{3}$$

In this case, there is no resonance. Clearly, A_{SR} is also monotonically decreasing with increasing Ω.

Now, add an external noise to the governing equation:

$$\frac{d}{dt}x = -\lambda x + a_0 \cos(\Omega t + \phi) + \tilde{g} \tag{4}$$

in which $\tilde{g}$ is zero mean, Gaussian, white noise with autocorrelation:

$$\langle \tilde{g}(t)\tilde{g}(t') \rangle = 2D\delta(t-t') . \tag{5}$$

D is the mean-square noise strength. We may think of $-\lambda x$ as the force caused by the parabolic potential $U = \frac{1}{2}\lambda x^2$. Since the dynamics only has the first-order time derivative, it is said to be "overdamped." More will be said about this feature below. Even for general U, the Fokker-Planck equation induced by the external noise is

$$\frac{\partial}{\partial t}P = \mathcal{L}P - \frac{\partial}{\partial x}a_0 \cos(\Omega t + \phi)P \tag{6}$$

where

$$\mathcal{L} = \frac{\partial}{\partial x}(U'\cdot) + D\frac{\partial^2}{\partial x^2} . \tag{7}$$

$\mathcal{L}$ is the Fokker-Planck operator and the dots indicate where to put the objects upon which it acts. Its eigenvalue-eigenfunction properties are

$$\mathcal{L}W = 0 \quad \text{with } W = N\exp\left[-\frac{U}{D}\right] , \tag{8}$$

where N is the normalization constant and

$$\mathcal{L}W\phi_n = -\lambda_n W\phi_n . \tag{9}$$

For the parabolic potential, these general equations yield

$$W=\left[2\pi\frac{D}{\lambda}\right]^{-1/2}\exp\left[-\frac{1}{2D}\lambda x^2\right], \tag{10}$$

$$\lambda_n=n\lambda, \tag{11}$$

$$\phi_n=(2^n n!)^{-1/2}H_n\left[\left[\frac{\lambda}{2D}\right]^{1/2}x\right], \tag{12}$$

in which H_n is the standard Hermite polynomial of order n. In particular we have $\lambda_1=\lambda$ and $\phi_1=(\lambda/D)^{1/2}x$. The position autocorrelation is computed with respect to both $\tilde{g}$ and ϕ. That is, we compute $\{\langle x(t)x(t')\rangle\}$ wherein $\langle\ \rangle$ denotes averaging with respect to $\tilde{g}$. The Fourier transform is taken to obtain $A_{\rm SR}$. We will show in Sec. II of this paper that for arbitrary potential U, to order a_0^2, $A_{\rm SR}$ is given by

$$A_{\rm SR}=\frac{\pi}{2}a_0^2\sum_{n=1}^{\infty}\sum_{m=1}^{\infty}\frac{\lambda_n\lambda_m(\lambda_n\lambda_m+\Omega^2)(\langle x\rangle_n)^2(\langle x\rangle_m)^2}{D^2(\lambda_n^2+\Omega^2)(\lambda_m^2+\Omega^2)}, \tag{13}$$

where $\langle x\rangle_n$ is defined by

$$\langle x\rangle_n=\int_{-\infty}^{\infty}dx\,xW(x)\phi_n(x). \tag{14}$$

At first sight this expression seems rather more complicated than (3). However, for the special case of the parabolic potential, it simplifies greatly because

$$\langle x\rangle_n=\left[\frac{D}{\lambda}\right]^{1/2}\delta_{n1} \tag{15}$$

so that

$$A_{\rm SR}=\frac{\pi}{2}a_0^2\frac{1}{\lambda^2+\Omega^2}. \tag{16}$$

This is identical to (3) and, remarkably, independent of D. The D independence is by virtue of a perfect cancellation of factors of D. In the general case, we expect complicated D dependence because of more complicated, noncanceling D dependence in $\langle x\rangle_n$ and λ_n.

The double-well potential $U=-\frac{1}{2}x^2+\frac{1}{4}x^4$ gives an example of complicated D dependence. This potential is the prototype for stochastic resonance. The governing equation is

$$\frac{d}{dt}x=x-x^3+a_0\cos(\Omega t+\phi)+\tilde{g}. \tag{17}$$

If this is viewed as overdamped motion in the double-well potential, then it must be noted that the external noise $\tilde{g}$ is not the noise connected with the damping constant through the fluctuation-dissipation relation. To see this, imagine that the underlying dynamics is

$$m\frac{d^2}{dt^2}x=-R\frac{d}{dt}x+(x-x^3)+\tilde{G} \tag{18}$$

where

$$\langle\tilde{G}(t)\tilde{G}(t')\rangle=2Rk_BT\delta(t-t') \tag{19}$$

expresses the fluctuation-dissipation relation. T is the temperature and K_B is Boltzmann's constant. Writing (18) as

$$\frac{m}{R}\frac{d^2}{dt^2}x+\frac{d}{dt}x=\frac{1}{R}(x-x^3)+\frac{1}{R}\tilde{G} \tag{20}$$

makes it patent that in the scaled time $\tau=t/R$

$$\frac{d}{d\tau}x=(x-x^3)+\tilde{G}(R\tau) \tag{21}$$

in the overdamped ($R\to\infty$) limit. Moreover, the noise autocorrelation now reads

$$\langle\tilde{G}(R\tau)\tilde{G}(R\tau')\rangle=2k_BT\delta(\tau-\tau'), \tag{22}$$

i.e., the noise correlation, in scaled time, is R times smaller than before, but not vanishing. In a real experiment, the residual internal noise must be accounted for when external noise $\tilde{g}$ is added.

Unlike the parabolic case in which explicit, closed-form expressions exist for all λ_n's and all ϕ_n's, the double-well analysis does not go through so easily. Highly accurate numerical construction of finite sets of λ_n and ϕ_n is possible using matrix continued fractions [6]. Jung [7] has pioneered and implemented this procedure for the double-well potential. He presented the first, highly accurate, published computation of $A_{\rm SR}$ [8]. The $A_{\rm SR}$ profile (for $\Omega=0.1$) is shown in Fig. 1 [we have plotted $(2/\pi a_0^2)A_{\rm SR}$ instead of $A_{\rm SR}$]. For fixed Ω, the profile shows a maximum as a function of D at $D=D_M$. In the parabolic case, $(2/\pi a_0^2)A_{\rm SR}$ was independent of D, with the constant value $1/(1+\Omega^2)$ which is less than 1 (having set $\lambda=1$ as we said we would earlier). The maximum in Fig. 1 has a value larger than 12. In this sense we have a "resonance" with respect to D at $D=D_M$. Notice that this phenomenon does not imply that $A_{\rm SR}$ has a maximum as a function of Ω for fixed D. In fact, for fixed D, $A_{\rm SR}$ is monotonically decreasing with increasing Ω.

With the double-well potential, a new time scale ap-

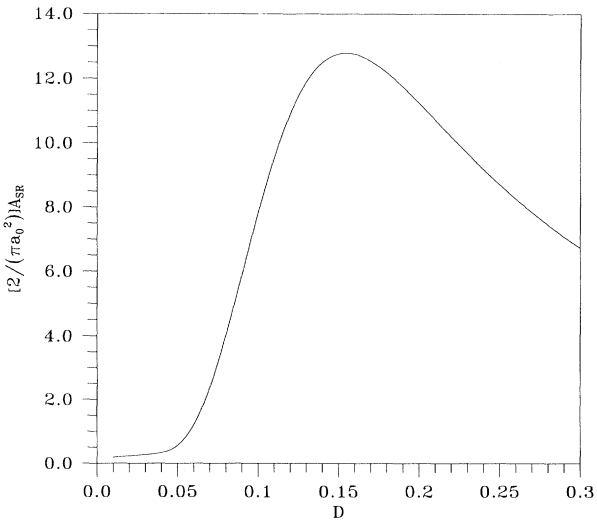

FIG. 1. $(2/\pi a_0^2)A_{\rm SR}$ for $\Omega=0.1$ and $D\in[0.01,0.3]$ redrawn from [4].

pears, the mean first-passage time (FPT) for the particle to hop from one minimum to the other. There exists a moment hierarchy of mean FPT, mean squared FPT, mean cubed FPT, etc. Each such moment depends on both the starting point and on the ending point, as well as on D. In this paper, we will be especially interested in the mean FPT to go from -1 to 0, $T_1(-1,0,D)$, and the mean squared FPT, $T_2(-1,0,D)$. The D dependence is of central interest.

Jung and Hanggi made the remarkable observation that D_M has an additional significance. Let D_R denote the value of D for which

$$T_1(-1,1,D_R)=\frac{1}{2}\frac{2\pi}{\Omega} . \tag{23}$$

For this value of D, the stochastic hopping period to go from -1 to $+1$ and back to -1 exactly equals the modulation period $2\pi/\Omega$. Jung and Hanggi [8,9] observed that

$$D_R=D_M , \tag{24}$$

which, for this phenomenon, confers a dramatic alternative sense to the word "resonance."

We tested this claim by determining D_M from Fig. 2 of Jung and Hanggi [8], and then using this D_M in a stochastic, numerical simulation [10,11], which determines $T_1(-1,1,D_M)$. For $\Omega=0.1$, the agreement with (24) was remarkably good. It is not unusual to hear the equivalent of (24) given as the explanation for stochastic resonance [8,9,12].

Identity (24) poses the following puzzles. Can $D_R=D_M$ be deduced analytically from general formula (13)? Can it readily be seen that the factors in (13) are connected with the mean FPT, $T_1(-1,1,D)$?

A tantalizing clue is the often stated approximate connection [6,8]

$$\lambda_1=\frac{1}{T_1(-1,0,D)} \tag{25}$$

for small enough D. Furthermore, the explicit D dependence is reasonably well approximated by the Kramers formula: $\lambda_1=(\sqrt{2}/\pi)\exp[-1/4D]$. These facts make it seem very likely that (24) could be obtained from (13) as a formal identity.

In Sec. II, we present the details required to obtain (13) and establish connections closely related to (25). We will show that the condition for stochastic resonance, (24), is only approximately true for $\Omega=0.1$ and gets worse as Ω is decreased. Instead, a remarkably good equation for determining $D_M(\Omega)$ is given by what we will call the Kramers condition

$$D_M(\Omega)=\frac{1}{4}\frac{1}{1+\dfrac{2\exp\left[-\left[\dfrac{1}{2D_M}\right]\right]}{\pi^2\Omega^2}} , \tag{26}$$

a transcendental equation for D_M. Only for a particular value of Ω, a bit larger than 0.1, is $D_R=D_M$ exactly true, by accident. Otherwise, the difference becomes increasingly significant as Ω decreases.

In Sec. III, we present our numerical results and confirm the validity of the Kramers condition (26). We also present concluding remarks.

II. DERIVATION OF A_{SR}

For the double-well potential, the Fokker-Planck equation is identical with (6) with the Fokker-Planck operator given by (7) with $U=-\frac{1}{2}x^2+\frac{1}{4}x^4$ in this case. The eigenvalue-eigenfunction equation

$$\mathcal{L}\psi=-\lambda\psi \tag{27}$$

cannot be solved in closed form, but there are several accurate, approximate approaches that are useful. Clearly, (8) still holds with

$$N^{-1}=\int_{-\infty}^{\infty}dx\,\exp\left[\frac{x^2}{2D}-\frac{x^4}{4D}\right] . \tag{28}$$

One may solve the eigenvalue-eigenfunction problem in the "backward" picture:

$$\mathcal{L}W\phi_n=-\lambda_n W\phi_n , \tag{29}$$

which is equivalent to saying that the ϕ_n's satisfy the backward Fokker-Planck equation [13]. This means the orthonormality and closure are expressed by

$$\int_{-\infty}^{\infty}dx\,\phi_n(x)W(x)\phi_m(x)=\delta_{nm} \tag{30}$$

and

$$\sum_{n=0}^{\infty}W(x)\phi_n(x)\phi_n(x')=\delta(x-x') . \tag{31}$$

The asymmetry in x and x' on the left-hand side of (31) corresponds to the conventions: for arbitrary $f(x)$, the eigenfunction expansion is

$$f(x)=\sum_{n=0}^{\infty}b_n W(x)\phi_n(x) \tag{32}$$

with coefficient formula

$$b_n=\int_{-\infty}^{\infty}dx\,\phi_n(x)f(x) . \tag{33}$$

Therefore, the δ function defined in (31) is properly two sided:

$$\int_{-\infty}^{\infty}dx'\delta(x-x')f(x')=f(x) \tag{34}$$

and

$$\int_{-\infty}^{\infty}dx\,\phi_n(x)\delta(x-x')=\phi_n(x') . \tag{35}$$

(Note that $\mathcal{L}$ is not Hermitian in this backward picture [14].)

The following identity is especially useful later:

$$\mathcal{L}W\phi_n=D\frac{\partial}{\partial x}W\frac{\partial}{\partial x}\phi_n=-\lambda_n W\phi_n . \tag{36}$$

This implies:

$$-\lambda_n \int_{-\infty}^{\infty} dx\ \phi_n W \phi_n = \int_{-\infty}^{\infty} dx\ \phi_n \mathcal{L} W \phi_n$$
$$= \int_{-\infty}^{\infty} dx\ D\phi_n \frac{\partial}{\partial x} W \frac{\partial}{\partial x} \phi_n$$
$$= -D \int_{-\infty}^{\infty} dx\ W(x) \left[\frac{\partial}{\partial x} \phi_n \right]^2 \leq 0 \ . \tag{37}$$

Therefore,

$$\lambda_n \geq 0 \quad \text{for every } n \ . \tag{38}$$

The solution to the full Fokker-Planck equation (6) utilizes the expansion

$$P(x,t;y,t',\phi) = \sum_{n=0}^{\infty} c_n(t,t',y,\phi) W(x) \phi_n(x) \tag{39}$$

in which P is the conditional probability density, such that $P\,dx$ is the probability for the position to be between x and $x+dx$ at time t given that the position value was precisely y at time t', all of this with phase ϕ. The formal solution to (6) is expressed as

$$c_n(t,t',y,\phi) = \left[\exp_T \left[\int_{t'}^{t} ds [\mathcal{L} - g(s)\mathcal{M}] \right] \right]_{nm} \phi_m(y) \tag{40}$$

wherein $\exp_T$ denotes the leftward, time-ordered exponential, with later times to the left, summation over the repeated m is implicit, and $\mathcal{M}$ is defined by

$$M_{nm} = (\mathcal{M})_{nm} = \int_{-\infty}^{\infty} dx\ \phi_n \frac{\partial}{\partial x} W \phi_m \tag{41}$$

and

$$g(s) = a_0 \cos(\Omega s + \phi) \ . \tag{42}$$

Clearly,

$$(\mathcal{L})_{nm} = \int_{-\infty}^{\infty} dx\ \phi_n \mathcal{L} W \phi_m = -\lambda_n \delta_{nm} \ . \tag{43}$$

It is known [6], and obvious, that $\lambda_0 = 0$ with $\phi_0 = 1$, and that $\lambda_n > 0$ for $n \geq 1$. Thus it is possible to obtain the asymptotic values for the c_n's. In particular, if we replace the upper limit t by t' and the lower limit t' by $-\infty$ in the integral on the right-hand side of (40), then we get

$$c_m^{\text{asy}}(t',\phi) = \left[\exp_T \left[\int_{-\infty}^{t'} ds [\mathcal{L} - g(s)\mathcal{M}] \right] \right]_{mp} \phi_p(y)$$
$$= \left[\exp_T \left[\int_{-\infty}^{t'} ds [\mathcal{L} - g(s)\mathcal{M}] \right] \right]_{m0} \tag{44}$$

because expansion of the ordered exponential and execution of all of the time integrals allows one to see that each term with $\lambda_p > 0$ in it vanishes. This means that

$$P^{\text{asy}}(y,t',\phi) = \sum_{m=0}^{\infty} c_m^{\text{asy}}(t',\phi) W(y) \phi_m(y) \tag{45}$$

can be used for the initial-value probability distribution for averaging over the initial position value y. In the unmodulated situation, this distribution is time independent, but not in this case in which the periodic modulation, with fixed phase ϕ, is applied forever. Thus there is ϕ dependence in P^{asy}. Nevertheless, (39) and (40) enable one to verify the Chapman-Kolmogorov identity which is a consistency requirement for a Markov process.

For a Markov process, the position autocorrelation function with respect to $\bar{g}$ is expressed [8,13] as

$$\langle x(t)x(t') \rangle = \int_{-\infty}^{\infty} dx \int_{-\infty}^{\infty} dy\ x\, P(x,t;y,t',\phi) y P^{\text{asy}}(y,t',\phi)$$
$$= \sum_{n=0}^{\infty} \sum_{m=0}^{\infty} c_n(t,t',y,\phi) \int_{-\infty}^{\infty} dx\ x W(x) \phi_n(x) c_m^{\text{asy}}(t',\phi) \int_{-\infty}^{\infty} dy\ y W(y) \phi_m(y) \ , \tag{46}$$

where the second equality follows from substitution of (39) and (45) into the first.

We are interested in the results for small a_0. By expanding c_n and c_m^{asy} to second order in a_0, rather complicated expressions are obtained. Nevertheless, a straightforward (albeit lengthy) calculation of the ϕ average makes the process stationary. This provides $\{\langle x(t)x(t') \rangle\}$, which only depends on $t-t'$, and the Fourier transform of which contains $\delta(\omega - \Omega)$. The coefficient A_{SR} is found to be, to second order in a_0,

$$A_{\text{SR}} = \frac{\pi}{2} a_0^2 \sum_{n=1}^{\infty} \sum_{m=1}^{\infty} \frac{M_{m0} M_{n0} (\lambda_n \lambda_m + \Omega^2) \langle x \rangle_n \langle x \rangle_m}{(\lambda_n^2 + \Omega^2)(\lambda_m^2 + \Omega^2)} \tag{47}$$

wherein $\langle x \rangle_n$ is defined by (14). We find from (14) that

$$\langle x \rangle_n = -\int_{-\infty}^{\infty} dx\ x \frac{\mathcal{L}}{\lambda_n} W \phi_n = \frac{1}{\lambda_n} \int_{-\infty}^{\infty} dx\ U' W \phi_n$$
$$= -\frac{D}{\lambda_n} \int_{-\infty}^{\infty} dx\ \phi_n \frac{\partial}{\partial x} W = -\frac{D}{\lambda_n} M_{n0} \ . \tag{48}$$

This identity does not depend on the explicit form of U, only on the form of $\mathcal{L}$ in (7). Substitution of (48) into (47) produces the general formula (13).

Define $R(\Omega)$, a generalization of the response function introduced in [9], by

$$R(\Omega) = \frac{1}{D} \sum_{n=1}^{\infty} \frac{\lambda_n (\langle x \rangle_n)^2}{\lambda_n + i\Omega} \ . \tag{49}$$

Therefore,

$$A_{\text{SR}} = \frac{\pi}{2} a_0^2 |R(\Omega)|^2 \ . \tag{50}$$

Moreover, $R(\Omega)$ is the Fourier transform (at $\omega = \Omega$) of

$-(d/dt)K(t)$ where

$$K(t)=\frac{1}{D}\sum_{n=1}^{\infty}\exp(-\lambda_n t)(\langle x\rangle_n)^2 . \tag{51}$$

This expression has a simple interpretation. Imagine that there is no modulation, i.e., $a_0=0$. Setting $t'=0$ and $a_0=0$ in (44) implies

$$c_m^{\text{asy}}=\delta_{m0} . \tag{52}$$

Doing the same in (40) implies

$$c_n(t,0,y)=\exp(-\lambda_n t)\phi_n(y) . \tag{53}$$

Equation (46) becomes

$$\begin{aligned}\langle x(t)x(t')\rangle &= \sum_{n=0}^{\infty}\int_{-\infty}^{\infty}dy\, yW(y)\exp(-\lambda_n t)\phi_n(y)\\ &\quad\times\int_{-\infty}^{\infty}dx\, xW(x)\phi_n(x)\\ &=\sum_{n=0}^{\infty}\exp(-\lambda_n t)(\langle x\rangle_n)^2 .\end{aligned} \tag{54}$$

Thus $DK(t)$ is the position autocorrelation obtained in the absence of external modulation.

That A_{SR} is monotonically decreasing with increasing Ω can be seen from (13) by differentiation with respect to Ω, summand by summand, and application of the inequality $\lambda_n\lambda_m\le\lambda_n^2+\lambda_m^2$.

Connections between the mean FPT (and higher FPT moments) and D_M, the D value for which A_{SR} is maximum, are established as follows. Recall (36) and compare it with the equation for the mean FPT to go from x to 0, $T_1(x,0,D)$, which is [13]

$$DW^{-1}\frac{\partial}{\partial x}W\frac{\partial}{\partial x}T_1(x,0,D)=-1 , \tag{55}$$

with boundary conditions $T_1(0,0,D)=0$ (absorbing at 0) and $(\partial/\partial x)T_1(-\infty,0,D)=0$ (reflecting at $-\infty$). We will work in the interval $x\in(-\infty,0]$. The exact solution to (55) is

$$T_1(x,0,D)=\frac{1}{D}\int_x^0 dy\, W^{-1}(y)\int_{-\infty}^{y}dz\, W(z) . \tag{56}$$

An integral equation exactly equivalent to (36) is

$$\phi_n(x)=\phi_n(-1)-\frac{\lambda_n}{D}\int_{-1}^{x}dy\, W^{-1}(y)\int_{-\infty}^{y}dz\, W(z)\phi_n(z) \tag{57}$$

for $x<0$ and $\phi_n(x)=-\phi_n(-x)$ for $x>0$ if n is odd. [In (13) we only need expressions for the odd-parity states because of the ubiquitous appearance of $\langle x\rangle_n$ factors.] Equation (57) may be iterated to obtain an implicit infinite series solution to (36):

$$\begin{aligned}\phi_n(x)=\phi_n(-1)\Bigg[1&-\frac{\lambda_n}{D}\int_{-1}^{x}dy\, W^{-1}(y)\int_{-\infty}^{y}dz\, W(z)\\ &+\left[\frac{\lambda_n}{D}\right]^2\int_{-1}^{x}dy\, W^{-1}(y)\int_{-\infty}^{y}dz\, W(z)\int_{-1}^{z}dy' W^{-1}(y')\int_{-\infty}^{y'}dz' W(z')+\cdots\Bigg] .\end{aligned} \tag{58}$$

Similarly, the mean squared FPT, $T_2(x,0,D)$, satisfies the equation

$$DW^{-1}\frac{\partial}{\partial x}W\frac{\partial}{\partial x}T_2(x,0,D)=-T_1(x,0,D) , \tag{59}$$

with the same boundary conditions as for (55), and has the exact solution

$$T_2(x,0,D)=\frac{2}{D^2}\int_x^0 dy\, W^{-1}(y)\int_{-\infty}^{y}dz\, W(z)\int_z^0 dy' W^{-1}(y')\int_{-\infty}^{y'}dz' W(z') . \tag{60}$$

It is extremely important to notice the similarities and the differences (especially the integration limits) between (56) and (58) and between (58) and (60). The desired connection follows from the property of odd-parity states that $\phi_n(0)=0$ [6]. Imposing this on (58) produces the eigenvalue equation

$$1-\frac{\lambda_n}{D}\int_{-1}^{0}dy\, W^{-1}(y)\int_{-\infty}^{y}dz\, W(z)+\left[\frac{\lambda_n}{D}\right]^2\int_{-1}^{0}dy\, W^{-1}(y)\int_{-\infty}^{y}dz\, W(z)\int_{-1}^{z}dy' W^{-1}(y')\int_{-\infty}^{y'}dz' W(z')+\cdots=0 . \tag{61}$$

The roots of this equation are the eigenvalues with odd index n. When such a root is inserted into (58), the explicit solution, for odd n, is obtained. By adroitly manipulating the limits of integration, (61) can be rewritten [using the shorthand $T_1=T_1(-1,0,D)$ and $T_2=T_2(-1,0,D)$] with the help of (56) and (60)

$$1-T_1\lambda_n+(T_1^2-\tfrac{1}{2}T_2)\lambda_n^2+\cdots=0 . \tag{62}$$

The two lowest roots are

$$\lambda_1=\frac{1}{T_1}+\frac{T_1^2-\frac{1}{2}T_2}{T_1^3}+\cdots \tag{63}$$

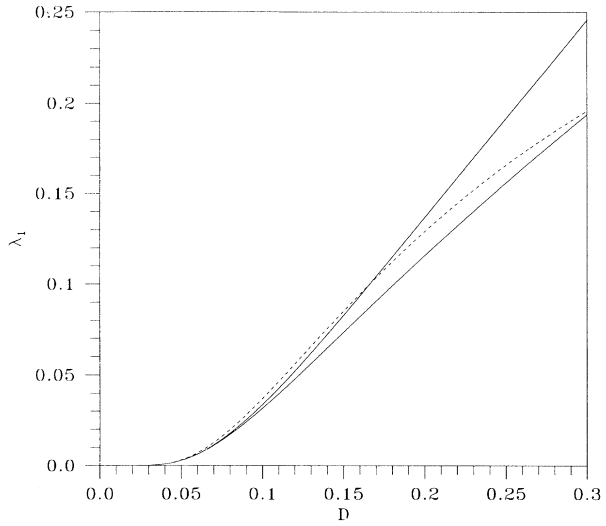

FIG. 2. The lower solid curve is the first-order approximation to (63) and the upper solid curve is the second-order approximation to (63) as functions of $D \in [0.01, 0.3]$. The dashed curve is the Kramers formula.

and

$$\lambda_3 = \frac{T_1}{T_1^2 - \frac{1}{2}T_2} - \lambda_1 \ . \tag{64}$$

These results are meaningful if the second term on the right-hand side of (63) is small. For the D values explored in this paper, this is the case, and it serves to confirm the rapid convergence of expression (58).

Several points need to be noted. For small enough D (in practice $D < 0.1$), the first term on the right-hand side of (63) is an excellent approximation, and this is the basis for the simple statement that the first nonzero eigenvalue is the reciprocal of the mean FPT. For $\Omega = 0.1$ and for D in the vicinity of D_M, the second term on the right-hand side of (63) is not ignorable, although still small (see Fig. 2). Also note that $T_1(-1,1,D) = T_1(-1,0,D) + T_1(0,1,D)$, but that $T_1(0,1,D) > T_1(-1,0,D)$, so that $T_1(-1,1,D) = 2T_1(-1,0,D)$ is only approximate. This is shown in Fig. 3. While the difference between $T_1(-1,1,D)$ and $2T_1(-1,0,D)$ is very small for the D values explored in this paper, we have nevertheless used $T_1(-1,1,D)$ in our assessment of (24).

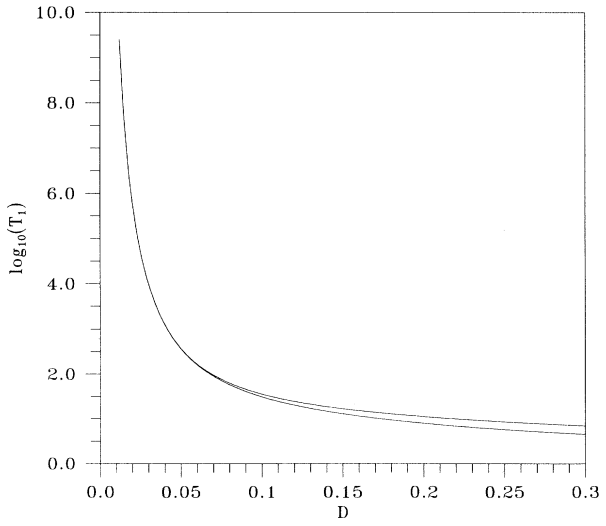

FIG. 3. The lower curve is $\log_{10}[T_1(-1,0,D)]$ and the upper curve is $\log_{10}[T_1(0,1,D)]$ as functions of $D \in [0.01, 0.3]$.

It may appear that we have barely begun to evaluate all of the λ_n's and ϕ_n's needed in (13), but it turns out that it is possible to find very good upper and lower bounds for $A_{\rm SR}$ that only depend on λ_1 and λ_3 and on $\phi_1(x)$ to the second order as given by (58). These bounds follow from the sum rule:

$$\begin{aligned}\langle x^2 \rangle &= \int_{-\infty}^{\infty} dx \int_{-\infty}^{\infty} dy\, xy W(x) \delta(y-x) \\ &= \int_{-\infty}^{\infty} dx \int_{-\infty}^{\infty} dy\, xy W(x) \sum_{n=1}^{\infty} W(y)\phi_n(y)\phi_n(x) \\ &= \sum_{n=1}^{\infty} \langle x \rangle_n \langle y \rangle_n = \sum_{n=1}^{\infty} (\langle x \rangle_n)^2 \\ &= (\langle x \rangle_1)^2 + \sum_{n=3}^{\infty} (\langle x \rangle_n)^2 \ . \end{aligned} \tag{65}$$

We may write $(2/\pi a_0^2) A_{\rm SR}$ in the form

$$\frac{2}{\pi a_0^2} A_{\rm SR} = S_1^2 + S_2^2 \ , \tag{66}$$

where

$$S_1 = \frac{1}{D} \sum_{n=1}^{\infty} \frac{\lambda_n^2 (\langle x \rangle_n)^2}{(\lambda_n^2 + \Omega^2)}, \quad S_2 = \frac{1}{D} \sum_{n=1}^{\infty} \frac{\Omega \lambda_n (\langle x \rangle_n)^2}{(\lambda_n^2 + \Omega^2)} \ . \tag{67}$$

The sum rule is used to obtain the inequalities as follows:

$$\begin{aligned} S_1 &= \frac{1}{D} \frac{\lambda_1^2 (\langle x \rangle_1)^2}{(\lambda_1^2 + \Omega^2)} + \frac{1}{D} \sum_{n=3}^{\infty} \frac{\lambda_n^2 (\langle x \rangle_n)^2}{(\lambda_n^2 + \Omega^2)} \\ &= \frac{1}{D} \frac{\lambda_1^2 (\langle x \rangle_1)^2}{(\lambda_1^2 + \Omega^2)} + \frac{1}{D} \sum_{n=3}^{\infty} \left[1 - \frac{\Omega^2}{(\lambda_n^2 + \Omega^2)} \right] (\langle x \rangle_n)^2 \\ &= \frac{1}{D} \frac{\lambda_1^2 (\langle x \rangle_1)^2}{(\lambda_1^2 + \Omega^2)} + \frac{1}{D} [\langle x^2 \rangle - (\langle x \rangle_1)^2] \\ &\quad - \frac{\Omega^2}{D} \sum_{n=3}^{\infty} \frac{(\langle x \rangle_n)^2}{(\lambda_n^2 + \Omega^2)} \ . \end{aligned} \tag{68}$$

Hence

$$S_1 \le \frac{1}{D} \frac{\lambda_1^2 (\langle x \rangle_1)^2}{(\lambda_1^2 + \Omega^2)} + \frac{1}{D} [\langle x^2 \rangle - (\langle x \rangle_1)^2] \ . \tag{69}$$

Since

$$\sum_{n=3}^{\infty}\frac{(\langle x\rangle_n)^2}{(\lambda_n^2+\Omega^2)}\le\frac{1}{\lambda_3^2+\Omega^2}\sum_{n=3}^{\infty}(\langle x\rangle_n)^2$$
$$=\frac{1}{\lambda_3^2+\Omega^2}[\langle x^2\rangle-(\langle x\rangle_1)^2]\,, \tag{70}$$

we also get

$$S_1\ge\frac{1}{D}\frac{\lambda_1^2(\langle x\rangle_1)^2}{(\lambda_1^2+\Omega^2)}+\frac{1}{D}\frac{\lambda_3^2}{(\lambda_3^2+\Omega^2)}[\langle x^2\rangle-(\langle x\rangle_1)^2]\,. \tag{71}$$

Because $\lambda_n\Omega\le\frac{1}{2}(\lambda_n^2+\Omega^2)$, we obtain

$$\frac{1}{D}\frac{\Omega\lambda_1(\langle x\rangle_1)^2}{(\lambda_1^2+\Omega^2)}\le S_2\le\frac{1}{D}\frac{\Omega\lambda_1(\langle x\rangle_1)^2}{(\lambda_1^2+\Omega^2)}$$
$$+\frac{1}{2D}[\langle x^2\rangle-(\langle x\rangle_1)^2]\,. \tag{72}$$

Therefore, we get the bounds

$$\frac{1}{D^2}\left[\frac{\lambda_1^2(\langle x\rangle_1)^4}{(\lambda_1^2+\Omega^2)}+\left[\frac{\lambda_3^4}{(\lambda_3^2+\Omega^2)^2}[\langle x^2\rangle-(\langle x\rangle_1)^2]+\frac{2\lambda_1^2\lambda_3^2(\langle x\rangle_1)^2}{(\lambda_1^2+\Omega^2)(\lambda_3^2+\Omega^2)}\right][\langle x^2\rangle-(\langle x\rangle_1)^2]\right]$$
$$\le\frac{2}{\pi a_0^2}A_{\rm SR}\le\frac{1}{D^2}\left[\frac{\lambda_1^2(\langle x\rangle_1)^4}{(\lambda_1^2+\Omega^2)}+\left[\tfrac{5}{4}[\langle x^2\rangle-(\langle x\rangle_1)^2]+\frac{\lambda_1(2\lambda_1+\Omega)(\langle x\rangle_1)^2}{(\lambda_1^2+\Omega^2)}\right](\langle x^2\rangle-(\langle x\rangle_1)^2)\right]\,. \tag{73}$$

The upper bound involves only λ_1 and ϕ_1 whereas the lower bound also requires λ_3. These facts enormously simplify our numerical work.

III. NUMERICAL RESULTS

Figure 4 shows plots of the upper and lower bounds for $(2/\pi a_0^2)A_{\rm SR}$ for $\Omega=0.1$ and $D\in[0.01,0.3]$. Figure 5 shows the same for $\Omega=0.01$. For $\Omega=0.01$, note how much larger the $A_{\rm SR}$ value is at D_M. For $\Omega=0.1$, the agreement with Jung and Hanggi is excellent. In Table I, the D_M values for $\Omega\in[0.001,0.1]$ are presented. We note that

$$\frac{dD_M(\Omega)}{d\Omega}>0\,. \tag{74}$$

Also in Table I are the $D_R(\Omega)$ values determined by (23). The difference between D_M and D_R is relatively small, lending credence to (24). However, the exponential dependence of $T_1(-1,1,D)$ on D, suggested by the Kramers formula for λ_1 and by $T_1\sim 1/\lambda_1$, leads to much larger differences between $T_1(-1,1,D_M)$ and $T_1(-1,1,D_R)=\pi/\Omega$. Thus (24) is not true for arbitrary Ω. This is shown in Table II.

The procedure used to calculate the results just presented was to use (i) (56) and (60) to numerically compute T_1 and T_2; (ii) (63) and (64) to compute λ_1 and λ_3, or by directly finding the roots to (62) expanded to second order; (iii) (58) to compute $\phi_1(x)$, using $\lambda_n=\lambda_1$ from (ii); (iv) (14) to obtain $\langle x\rangle_1$; and (v) (73) to yield $A_{\rm SR}$ upper and lower bounds. We found that ϕ_1 was very well approximated by the double integral in (58) and that inclusion of the fourth-order integral only made very small

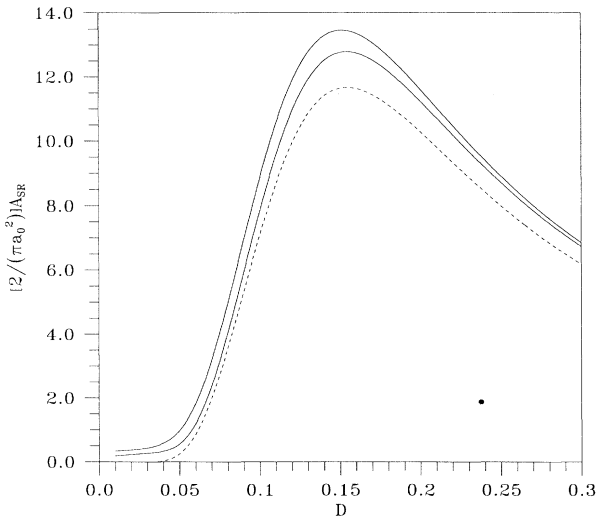

FIG. 4. The solid curves are the upper and lower bounds (73) for $(2/\pi a_0^2)A_{\rm SR}$ for $\Omega=0.1$ and $D\in[0.01,0.3]$. The dashed curve is simply the $n=1$ term in (13).

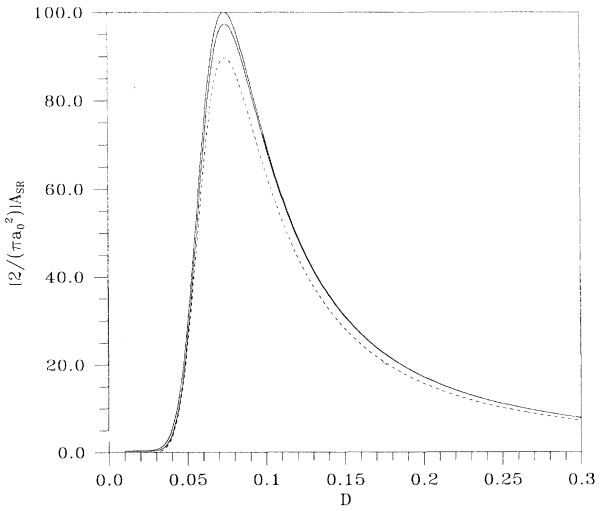

FIG. 5. Same as in Fig. 4, except that $\Omega=0.01$.

TABLE I. The first column is the frequency Ω, the second column is the D_M value determined from the upper bound in (73), the third column is the D_M determined from the lower bound, the fourth column is the D_R determined by (23), and the fifth column is the D_M value determined from the Kramers condition (26).

Ω	$\overline{D_M}$	$\underline{D_M}$	D_R	D_M
0.001	0.047	0.047	0.0385	0.0465
0.002	0.053	0.053	0.0432	0.0526
0.003	0.057	0.057	0.0466	0.0568
0.004	0.060	0.061	0.0493	0.0602
0.005	0.063	0.064	0.0516	0.0632
0.006	0.066	0.066	0.0537	0.0657
0.007	0.068	0.069	0.0556	0.0681
0.008	0.070	0.071	0.0573	0.0702
0.009	0.072	0.073	0.0590	0.0722
0.010	0.074	0.075	0.0605	0.0741
0.020	0.089	0.090	0.0734	0.0888
0.030	0.100	0.101	0.0838	0.0998
0.040	0.109	0.111	0.0933	0.1091
0.050	0.117	0.119	0.1023	0.1171
0.060	0.125	0.127	0.1110	0.1244
0.070	0.132	0.134	0.1195	0.1310
0.080	0.139	0.141	0.1279	0.1370
0.090	0.145	0.148	0.1363	0.1427
0.100	0.151	0.154	0.1447	0.1479

changes. We also tested our numerical integration of (56) against a stochastic simulation [10] and found better than 1% agreement.

For very small D, $A_{\rm SR}$ does not vanish. This fact, observed in [8,9], and explained with a phenomenological argument, is, for us, a systematic consequence of the λ_3 terms in (13) and (73). The leading term in both the upper and lower $A_{\rm SR}$ bounds

$$A^*_{\rm SR} \sim \frac{\pi}{2} a_0^2 \frac{1}{D^2} \frac{\lambda_1^2 (\langle x \rangle_1)^2}{(\lambda_1^2 + \Omega^2)} \tag{75}$$

does vanish for vanishing D. This is evident from the Kramers formula so that

$$\lim_{D \to 0} A^*_{\rm SR} \sim \frac{\pi}{2} a_0^2 \frac{\lambda_1^2}{D^2} \frac{1}{\Omega^2} \sim \frac{\exp\left[-\frac{1}{2D}\right]}{D^2} . \tag{76}$$

However, near the maximum, at D_M, (75) is a very good approximation for determining D_M because the two bounds on $A_{\rm SR}$ are so close together (see Figs. 4 and 5). If we use (75) together with the Kramers formula for λ_1, then we obtain (see below) the "Kramers condition" for D_M, already given in (26). Also shown in Table I is the D_M value determined by the Kramers condition (26). The agreement is remarkable, especially for small D, i.e., $D \leq 0.1$ (this is the region defined by $\Omega \leq 0.03$).

The qualitative features overall, and the quantitative features of the maximum associated with $A_{\rm SR}$ at $D = D_M$, are modeled very well by the simple expression (75), especially so for $\Omega \leq 0.03$. By comparing (75) with (16), an appreciation for the dynamical basis for stochastic resonance can be reached. Two factors are important: (i) the properties of λ_1 and (ii) the properties of $\langle x \rangle_1$.

For the parabolic potential, $\lambda_1 = \lambda$. The conditional probability distribution $P(x,t;y,t',\phi)$ relaxes with the time scales $1/\lambda_n = 1/n\lambda$, the slowest of which is associated with λ_1. There is no sharp separation of time scales between the faster ones and the slowest one. There is no D dependence in λ_1. The distribution settles down to a small-amplitude oscillation about the parabolic minimum. For the double-well potential, the asymptotic time distribution describes small-amplitude oscillations

TABLE II. The first column is the frequency Ω, the second column is $T_1(-1,1,D)$ determined from the second column of Table I, the third column is $T_1(-1,1,D)$ determined from the third column of Table I, and the fourth column is simply the right-hand side of (23).

Ω	$T_1(-1,1,\overline{D_M})$	$T_1(-1,1,\underline{D_M})$	$T_1(-1,1,D_R)$
0.001	996.3	996.3	3141.6
0.002	554.1	554.1	1570.8
0.003	402.0	402.0	1047.2
0.004	352.3	304.6	785.40
0.005	268.7	253.2	628.32
0.006	226.0	226.0	523.60
0.007	203.1	193.0	448.80
0.008	183.7	175.1	392.70
0.009	167.1	159.7	349.07
0.010	152.8	146.3	314.16
0.020	88.88	86.29	157.08
0.030	66.27	64.73	104.72
0.040	54.43	52.32	78.540
0.050	46.83	45.24	62.832
0.060	41.03	39.80	52.360
0.070	37.01	36.00	44.880
0.080	33.69	32.85	39.270
0.090	31.30	30.22	34.907
0.100	29.22	28.28	31.416

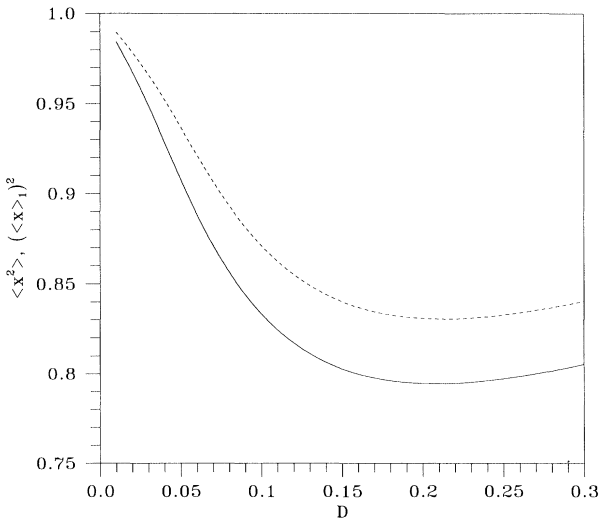

FIG. 6. The dashed curve is $\langle x^2 \rangle$ and the solid curve is $(\langle x \rangle_1)^2$, as functions of D.

about a bimodal distribution with equal densities concentrated at $+1$ and -1. The relaxation to this asymptotic state requires equilibration between the two probability maxima, which takes place on the time scale given by $T_1(-1,1,D)$ since hopping between potential minima is required. For small D, this is nearly the same as $2/\lambda_1$, as we have already seen, and $\lambda_1 \cong (\sqrt{2}/\pi)\exp[-1/4D]$. Thus there is a sharp separation of time scales, since $\lambda_1 \ll \lambda_n$ for $n \geq 2$ [6]. These facts bring $T_1(-1,1,D)$ into the picture.

The differences between the two cases is also marked for $\langle x \rangle_1$. For the parabolic potential, the maximum probability density is located around $x=0$. Consequently, $\langle x \rangle_1$ vanishes as $D \to 0$, since the probability density approaches a Dirac δ function around $x=0$. In fact, $\langle x \rangle_1 \to 0$ as $D \to 0$, as given by (15) so that there is an exact cancellation of D and λ factors in A_{SR} [see (16)]. For the double-well potential, however, the probability density is concentrated around both $+1$ and -1 equally, and in the limit $D \to 0, \langle x \rangle_1 \to 1$. This is shown in Fig. 6. The overall factor λ_1^2/D^2 is retained for $\Omega \leq 0.03$ (i.e., $D \to 0$) rather than perfectly canceling with $(\langle x \rangle_1)^4$, as it does for the parabolic potential.

These differences exhibit the importance of the role of $\langle x \rangle_1$ in the differences in the A_{SR}'s for the parabolic and double-well potentials. They show that for $\Omega \leq 0.03$ the value of D_M is very accurately determined by the approximation to A_{SR}, which is excellent for determining D_M:

$$A_{\mathrm{SR}} \sim \frac{\pi}{2} a_0^2 \frac{1}{D^2} \frac{\lambda_1^2}{(\lambda_1^2+\Omega^2)} . \tag{77}$$

When the Kramers formula for λ_1 is used, differentiation of this approximation with respect to D yields (26), the Kramers condition for D_M.

ACKNOWLEDGMENTS

This work was supported by NSF Grant No. PHY-9203878 and by the State Education Commission of the People's Republic of China.

*Permanent address: Institute of Low Energy Nuclear Physics, Beijing Normal University, Beijing 100875, People's Republic of China.

[1] R. Benzi, A. Sutera, and A. Vulpiani, J. Phys. A **14**, L453 (1981); R. Benzi, G. Parisi, A. Sutera, and A. Vulpiani, Tellus **34**, 10 (1982); R. Benzi, A. Sutera, and A. Vulpiani, SIAM (Soc. Ind. Appl. Math.) J. Appl. Math. **43**, 565 (1983).
[2] S. Fauve and F. Heslot, Phys. Lett. **97A**, 5 (1983).
[3] B. McNamara, K. Wiesenfeld, and R. Roy, Phys. Rev. Lett. **60**, 2626 (1988).
[4] J. Stat. Phys. **70** (1/2) (1992).
[5] B. McNamara and K. Wiesenfeld, Phys. Rev. A **39**, 4854 (1989).
[6] H. Risken, *The Fokker-Planck Equation,* 2nd ed. (Springer-Verlag, Berlin, 1989), Chap. 5.
[7] P. Jung, Z. Phys. B **76**, 521 (1989).
[8] P. Jung and P. Hanggi, Phys. Rev. A **44**, 8032 (1991).
[9] P. Jung and P. Hanggi, Z. Phys. B **90**, 255 (1993).
[10] R. F. Fox, Phys. Rev. Lett. **62**, 1205 (1989).
[11] R. F. Fox, Phys. Rev. A **43**, 2649 (1991).
[12] C. Presilla, F. Marchesoni, and L. Gammaitoni, Phys. Rev. A **40**, 2105 (1989); D. Leonard, *ibid.* **46**, 6742 (1992).
[13] C. Gardiner, *Handbook of Stochastic Methods* (Springer-Verlag, Berlin, 1983), Chap. 5.
[14] H. Gang, G. Nicolis, and C. Nicolis, Phys. Rev. A **42**, 2030 (1990).